Soft Matter

Non-dependence of Dodecamer Structures on Alkyl Chain Length in Platonic Micelles

Journal:	*Soft Matter*
Manuscript ID	SM-ART-01-2019-000076.R2
Article Type:	Paper
Date Submitted by the Author:	25-Feb-2019
Complete List of Authors:	Sakurai, Kazuo ; University of Kitakyushu, Dep. of Chemistry & Biochemistry Fujii, Shota; University of Kitakyushu, Araki, Masataka; Univ. Kitakushu Lee, Ji Ha; Univ. Kitakyushu Takahashi, Rintaro; Univ. Kitakyushu

Journal Name

ARTICLE

Non-dependence of Dodecamer Structures on Alkyl Chain Length in Platonic Micelles

Masataka Araki†, Shota Fujii†, Ji Ha Lee, Rintaro Takahashi, and Kazuo Sakurai*

Received 00th January 20xx,
Accepted 00th January 20xx

DOI: 10.1039/x0xx00000x

www.rsc.org/

When the micellar aggregation number (N_{agg}) is sufficiently small (N_{agg} < 30), the micelle shows an abnormal aggregation behavior: monodispersity without any distribution in N_{agg}, whose values coincide with the vertex number of a regular polyhedral structure, i.e., it is termed Platonic solids. Micelles with these characteristics are named "Platonic micelles." In this study, we investigated the aggregation behavior of calixarene-based micelles bearing primary amines—the first example of Platonic micelles—with increasing alkyl chain length by small-angle X-ray scattering, asymmetrical flow field flow fractionation coupled with multiangle light scattering, and analytical ultracentrifugation measurements. Morphological transition of the micelles from spherical to cylindrical was observed when the alkyl chain length was increased in this calixarene-based micellar system, which is similar to the case of conventional systems and is acceptable in terms of the packing parameter principle. However, although the micellar N_{agg} normally increases with an increase in the alkyl chain length, the structure of calixarene-based Platonic micelles bearing butyl (C4), heptyl (C5), and hexyl (C6) chains remains at 12-mer. This is presumably due to the relationship between the thermodynamic stability of the Platonic micelles and the coverage ratio defined by the Tammes problem.

Introduction

The fundamental science of conventional micelles has long been studied, and their theory, structures, formation mechanism, etc., are well understood in general.[1-6] According to the packing parameter theory, the micelle structure can be predicted to some extent using the packing parameters defined by $V/a_e h$, where a_e, V, *and* h are the equilibrium interfacial area between the hydrophilic and hydrophobic domains, volume of the surfactant, and length of the surfactant tail, respectively.[2] The a_e value and the aggregation number (N_{agg}) of micelles are also closely related and associated with the equation $N_{agg} \sim (4\pi h^2/a_e)$, meaning that N_{agg} decreases as a_e increases. This concept is widely accepted and well supported both experimentally and theoretically in various micelle systems.[7-14]

Micelles reported so far are not completely monodisperse, and their N_{agg} value is large. However, it has recently been demonstrated that when N_{agg} becomes as small as possible (that is, when the surfactant in the micelle has a large hydrophilic group, or if a_e is large), the micelle shows perfect monodispersity without any distribution in N_{agg}.[15-17] More interestingly, the N_{agg} value is always consistent with the face or vertex number of regular polyhedral structures (i.e., Platonic solids). Because of this structural characteristic, such micelles are named Platonic micelles (Figure 1).[18-22]

The major reason for the formation of Platonic micelles is suggested to the Tammes problem, which is one of the unresolved mathematical problems.[23-24] The Tammes problem considers a closest packing structure when placing a certain number of identical spherical caps on a sphere. The coverage ratio [$D(N)$] determined when the sphere is effectively covered by the spherical caps strongly depends on the spherical cap number (N); in particular, when N takes a value of 20 or smaller, a zigzag profile is obtained, as shown in Figure S1. $D(N)$ shows the local maxima when N matched the Platonic number. The micellar structure is spontaneously formed in aqueous solutions, where the hydrophilic part must effectively cover the hydrophobic core in order to minimize the interfacial free energy between the hydrophobic domain and the water interface. When the micelle has a very small N_{agg} (<30), it is considered that the closest packing structure, similar to the Tammes problem, is formed in the system. In this case, the micelle would be thermodynamically unstable when the hydrophobic core is exposed to the water interface; hence, Platonic micelles, whose N_{agg} is associated with a high $D(N)$ and corresponds to Platonic numbers, are spontaneously formed.

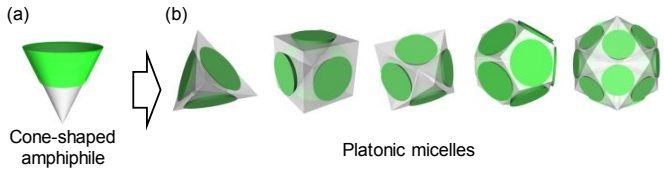

Figure 1. Schematic illustrations of cone-shaped amphiphiles (a) and Platonic micelles (b) including tetrahedral, hexahedral, octahedral, dodecahedral, and icosahedral structures. The green and gray parts indicate the hydrophilic and hydrophobic moieties, respectively.

Calixarenes are useful building blocks of amphiphilic molecules for producing Platonic micelles[25] because the cone-shaped structure provides large headgroups, which in turn confer a large a_e. It has been reported that a calixarene-based amphiphile containing primary amino groups in the hydrophilic

Department of Chemistry and Biochemistry, University of Kitakyushu, 1-1 Hibikino, Kitakyushu, Fukuoka 808-0135, Japan
† These authors contributed equally to this work.
Electronic Supplementary Information (ESI) available: [details of any supplementary information available should be included here]. See DOI: 10.1039/x0xx00000x

part and propyl tails in the hydrophobic part forms completely monodisperse hexameric micelles.[18] The N_{agg} value of the micelles increases to 12 when hexyl tails are attached instead of propyl tails. In this study, we identified a unique aggregation behavior related to the thermodynamic stability of Platonic micelles when the number of carbons in the alkyl chain is progressively increased in the calixarene-based micelle.

Results and Discussion

The calixarene-based amphiphile bearing primary amines in the head group and alkyl chains as the hydrophobic part (referred to as PACaL*n*) was synthesized via the reaction depicted in Scheme 1. The chemical structure was confirmed by ^{1}H-NMR spectroscopy at each synthesis step, and the molecular weight of the final product was confirmed by ESI-MS analysis (see Supporting information). The calixarene-based amphiphile stabilizes in the C_{4v} symmetry by enclosing a sodium ion in its calixarene cavity, and the micelle assumes a uniform structure owing to its highly symmetrical nature.[18] In addition, the amino group in PACaL*n* protonates under acidic conditions, which contributes to the formation of the cone-shaped conformation due to electrostatic repulsions among the protonated amines in the head group. This results in a large a_e, leading to the formation of Platonic micelles. Because of these properties, all the experiments were conducted using 50 mM aqueous NaCl at pH 3.0 as the solvent.

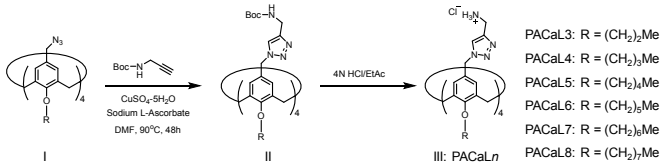

Scheme 1. Click chemistry-based synthetic route to primary amines bearing calixarene-based amphiphiles (PACaL*n*) with different alkyl chain lengths.

Figure 2a shows the SAXS profile of the PACaL*n* micelles in 50 mM aqueous NaCl (pH 3.0). In the profile of PACaL3, 4, 5, and 6, the slope on the low-q (q is the magnitude of the scattering vector defined as $q = (4\pi/\lambda)\sin(\theta/2)$ with a scattering angle θ.) side asymptotically approaches q^0, indicating the presence of isolated spherical micelles in the solution. Note that the sharpness of the first minimum in the SAXS oscillation indicates the monodispersity of the N_{agg} as well as the micellar size.[26-27] In the case of PACaL7 and 8, the slope in the low-q region is q^{-1}, suggesting the formation of rod micelles. All the SAXS profiles can be reproduced with the theoretical curves calculated using a core-shell spherical or cylindrical model; the fitting parameters are summarized in Table 1. In the scattering profile of PACaL*n* micelles that form spherical micelles, the minimum position in the oscillation gradually shifts to

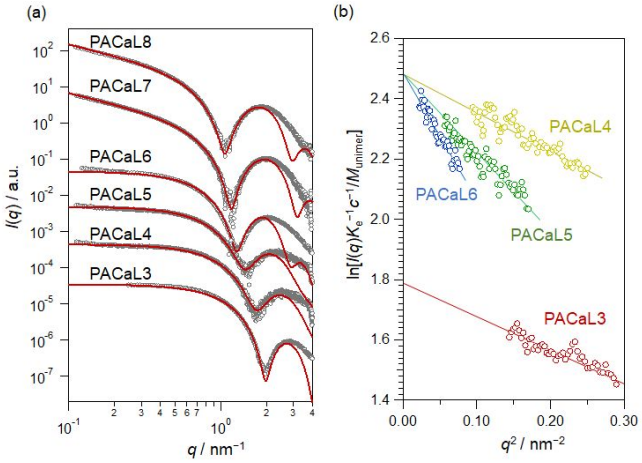

Figure 2. (a) SAXS profiles of PACaL*n* micelles (gray circles) in 50 mM aqueous NaCl (pH 3.0). The red curves are calculated using theoretical models of a sphere and a cylinder. (b) Guinier plots (i.e., ln $I(q)K_e^{-1}c^{-1}/M_{unimer}$ versus q^2, where K_e is an optical constant in SAXS) derived from the spherical micelles of PACaL*n*. (red: PACaL3, yellow: PACaL4, green: PACaL5, blue: PACaL6).

the lower-q side as the alkyl chain length increases. This indicates the micellar size increases with increasing alkyl chain length. The radius of the spherical micelles, estimated by fitting, also increases with the lengthening of the alkyl chain, and the radius of gyration (R_g) determined from Guinier analysis (Figure 2b) also shows a similar trend. The morphological transition of the micelle from spherical to cylindrical when increasing the alkyl chain length can be understood by the packing parameter principle.[2]

The micellar molar masses are determined by Guinier analysis, as shown in Figure 2b. The intercept of the Guinier plot corresponds to the N_{agg} value of the micelle. The micellar N_{agg}s values for PACaL3, 4, 5, and 6 are determined to be 6, 12, 12, and 12, respectively. Surprisingly, for the PACaL4, 5, and 6 systems, although the micellar size increases with the lengthening of the alkyl chain, N_{agg} remains constant at 12.

Figure 3a shows the multi-angle light scattering coupled with asymmetric flow field flow fractionation (AF4-MALS) fractograms of the PACaL3, 4, and 5 micelles. The fractograms display a single sharp peak derived from the spherical micelles suggested by SAXS, while that of PACaL6 shows the presence of large aggregates (Figure S4). The SAXS profile of PACaL6 indicates the presence of an isolated particle without any large aggregates, implying that the aggregates detected in AF4 measurements are probably formed by the concentrated condition during the focusing process in the AF4 system. The overlapping in the light scattering (LS)

Table 1. SAXS Fitting Parameters and Radius of Gyration (R_g) for PACaL*n* Micelles in 50 mM Aqueous NaCl (pH 3.0)

Sample	$R_{c,\,sphere}$ [nm]	$R_{s,\,sphere}$ [nm]	$R_{c,\,cylinder}$ [nm]	$R_{s,\,cylinder}$ [nm]	ρ_c [e nm^{-3}]	σ/R_s	ρ_s [e nm^{-3}]	R_g [nm]
PACaL3	0.700	2.05	–	–	270	0.02	391	1.47±0.11
PACaL4	1.00	2.10	–	–	270	0.05	405	1.58±0.15
PACaL5	1.18	2.25	–	–	270	0.07	405	1.94±0.17
PACaL6	1.45	2.75	–	–	270	0.04	420	2.52±0.19
PACaL7	–	–	1.20	2.20	270	0.04	450	1.70±0.10 [a]
PACaL8	–	–	1.30	2.35	270	0.04	440	1.87±0.13 [a]

$R_{c,\,sphere}$ and $R_{s,\,sphere}$ are the radii of the core and shell of the spherical model, respectively. $R_{c,\,cylinder}$ and $R_{s,\,cylinder}$ are the cross-sectional radii of the core and shell of the cylindrical model, respectively. σ/R_s is polydispersity in the micellar size. ρ_c and ρ_s are the electron densities of the core and shell, respectively.
a: cross-sectional radius of gyration determined from cross-sectional Guinier plots (Figure S3)

Table 2. Micellar Molar Masses Determined by Different Methods and Aggregation Numbers of the Spherical Micelles of PACaL*n* in 50 mM Aqueous NaCl (pH 3.0)

Sample	SAXS	AF4-MALS		AUC			N_{agg}
	M_w [10^4 g mol^{-1}]	M_w [10^4 g mol^{-1}]	M_w/M_n	M_w [10^4 g mol^{-1}]	M_z/M_w	A_2 [10^{-3} mol mL^{-2} g]	
PACaL3	0.58±0.02	0.618±0.030	1.06	0.610±0.030	1.07	−9.30	6.0±0.2
PACaL4	1.31±0.10	1.34±0.01	1.02	1.33±0.02	1.00	−4.91	12.0±0.2
PACaL5	1.38±0.50	1.37±0.01	1.01	1.39±0.04	1.00	−5.54	12.0±0.2
PACaL6	1.44±0.16	–	–	1.47±0.05	1.10	−2.28	12.0±0.1

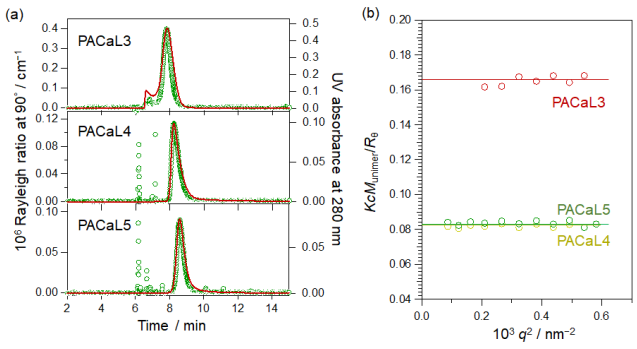

Figure 3. (a) AF4-MALS fractograms of PACaL*n* micelles in 50 mM NaCl aqueous solutions (pH 3.0). The green points and red lines are the Rayleigh ratio at 90° and UV absorbance at 280 nm, respectively. (b) Zimm plots [i.e., KcM_{unimer}/R_θ ($1/N_{agg}$) versus q^2] at the peak top in the AF4-MALS fractogram corresponding to the spherical micelles of PACaL*n*. (Red, yellow, and green indicate PACaL3, PACaL4, and PACaL5, respectively).

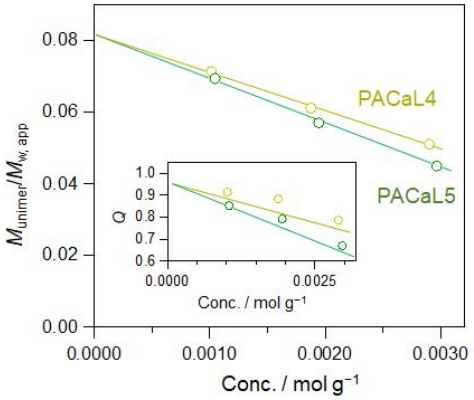

Figure 4. Concentration dependence of $M_{unimer}/M_{w,App}$ (i.e., $1/N_{agg}$ at Conc. = 0) determined by analytical ultracentrifugation measurements for PACaL*n* micelles in 50 mM aqueous NaCl (pH 3.0). (yellow: PACaL4, green: PACaL5). The inset shows the concentration dependence of Q (= $M_{w,App}/M_{z,App}$) for PACaL4 (yellow) and PACaL5 (green) micelles in 50 mM aqueous NaCl solutions (pH 3.0).

profiles depending on concentration and molecular weight, and that in the UV profile depending only on concentration imply that the scatterer molecular weight is constant in the overlapping regions. The LS and UV profiles overlap with each other almost completely for the PACaL4 and 5 systems, while they are slightly mismatched in the fractogram of PACaL3. The critical micelle concentration (CMC) of PACaL3 is 0.11 mM, which is relatively high compared to those of PACaL4 and 5 (Figure S5). Since the concentration of the PACaL3 micelle, determined from the UV absorbance in the fractogram, is very close to the value of CMC (Figure S6), the micellar stability is lower than that of the others, resulting in a slightly wider distribution than that of the other systems. However, the dispersity index (M_z/M_w) evaluated by analytical ultracentrifugation (AUC) at sufficiently higher concentrations than the CMC is close to 1.0,[18] indicating monodispersity; furthermore, the sharpness in the oscillation of the SAXS profile reveals the monodispersity of the PACaL3 micelle.

The Zimm plots at the peak top of the spherical micelles of PACaL3, 4, and 5 are shown in Figure 3b. The $I(0)$, which is the forward scattering intensity at q = 0, value obtained by extrapolating the plot to q = 0 corresponds to the inverse of the micellar N_{agg}. The N_{agg}s values of the spherical micelles of PACaL3, 4, and 5 determined from each $I(0)$ value are 6, 12, and 12, respectively, which is consistent with those determined by SAXS measurements.

The micellar N_{agg}s were confirmed another independent measurement based on AUC analysis. Figure 4 shows the concentration dependence of the micelle on the $M_{unimer}/M_{w,app}$ at centrifugation equilibrium state for the system of PACaL4 and 5. The intercept value corresponds to their N_{agg}, which is determined to be 12 for both systems. The N_{agg}s value of the micelles composed of PACaL3 and 6 have previously been determined to be 6 and 12, respectively, by AUC.[18] These values are summarized in Table 2. All the micellar N_{agg}s values estimated by three independent methods, i.e., SAXS, LS, and AUC, show good agreement with one another, leading us to conclude that N_{agg}s of the PACaL3, 4, 5, and 6 micelles is 6, 12, 12, and 12, respectively.

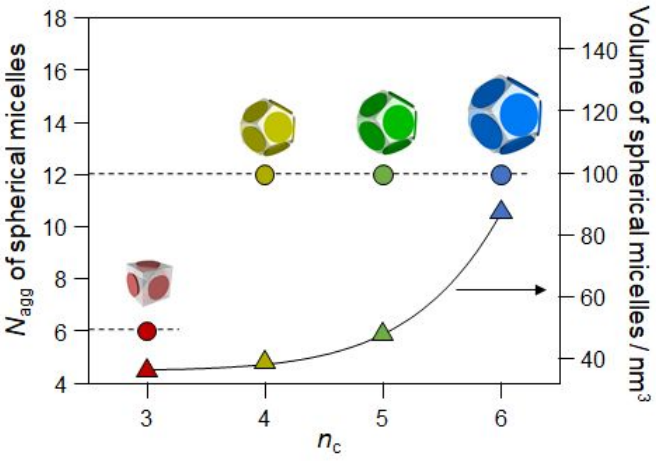

Figure 5. Dependence of N_{agg} (circle) and volume (triangle) estimated from R_s of the spherical micelles composed of PACaL*n* in 50 mM aqueous NaCl (pH 3.0) on alkyl chain length (n_c: number of carbons in each alkyl chain).

Though the all spherical micelles show a negative second virial coefficient (A_2), the PACaL3 micelle shows the lowest value

of A_2. This indicates that the hydrophobic core of the PACaL3 micelle is more exposed to the water interface, suggesting that its $D(N)$ is lower than that of the PACaL4, 5, and 6 micelles. The CMC of the PACaL3 micelle is larger than that of the other micelles (Figure S5), presumably because the structure of PACaL3 is more unstable due to the smaller $D(N)$.

In general micellar systems, N_{agg} increases with the lengthening of the alkyl chains, which leads to a morphological transition from spherical to cylindrical and then to plate-like. [28-29] However, in the PACaL4, 5, and 6 systems, N_{agg} does not depend on the length of the alkyl chain but retains its 12-mer (Figure 5), while the micellar morphology becomes rod-like when the alkyl chain length reaches C7, whose transition can be understood by packing parameter principle. As mentioned in the Introduction, the thermodynamic stability of Platonic micelles can be understood by $D(N)$, which is related to the Tammes problem. A higher $D(N)$ results in more stable structures, where the hydrophobic core would be well covered by the hydrophilic parts. According to this idea, in the $D(N)$ profile with a relatively small N_{agg}, the 12-mer confers the highest coverage (Figure S1), resulting in high stability. Hence, we believe that the 12-mer structure does not undergo structural transformation into micelles with other N_{agg} values, and that the most stable 12-mer structure is preserved even if the alkyl chain length is increased. Finally, the spherical structure is not retained because of the large packing parameter with longer alkyl chains (more than C7), resulting in structural transformation into rod-like micelles.

Conclusions

In conclusion, we prepared primary amines bearing calixarene-based amphiphiles (PACaL*n*) and investigated the effect of the alkyl chain length on the aggregation behavior by small-angle scattering techniques (SAXS and AF4-MALS) as well as AUC. When the alkyl chain is short enough to produce spherical micelles, the micelles show complete monodispersity in the aggregation numbers, whose values are consistent with the Platonic numbers. The micellar morphology changes to cylindrical at a certain chain length, which is a normal morphological transition due to the increasing packing parameter, as is often seemed in conventional systems. However, interestingly, when butyl (C4), heptyl (C5), and hexyl (C6) chains are introduced as the hydrophobic part in PACaL*n*, monodisperse 12-mer micelles are formed in all cases, which indicates the non-dependence of the structure on the alkyl chain length. This is attributable to the relationship between the thermodynamic micellar stability and the $D(N)$ value related to the Tammes problem. The alkyl chain length dependence for Platonic micelles shown in this study is abnormal, as opposed to the case of conventional micelles, implying the unique aggregation behavior of the micelle. In-depth understanding of the aggregation behavior of Platonic micelles is necessary for designing new self-assembling materials, and we hope that the present research will make a valuable contribution in this regard.

Experimental Section

Details of the synthesis of primary amines bearing calixarene-based amphiphiles and the characterization of micellar structures by small-angle scattering and analytical ultracentrifugation measurements are provided in Supporting information.

Conflicts of interest

There are no conflicts to declare.

Acknowledgements

We are grateful for the financial support from the JST/CREST program. All SAXS measurements were carried out at SPring-8 BL40B2 [2017A1414, 2017B1351, 2018A1454, 2018B1396]. This work was supported by JST CREST Grant Number JPMJCR1521, Japan, and a JSPS Grant-in-Aid for Scientific Research (B) (Grant Number 17K14073).

References

1. Tanford, C., The Hydrophobic Effect: Formation of Micelles and Biological Membranes 2nd ed. (Wiley-Interscience, 1980).
2. Israelachvili, J. N., Intermolecular and surface forces. Vol. 450 (Academic press London, 1992).
3. Nagarajan, R., *Langmuir* 2002, ***18*** (1), 31-38.
4. Jensen, G. V.; Lund, R.; Gummel, J.; Monkenbusch, M.; Narayanan, T.; Pedersen, J. S., *J. Am. Chem. Soc.* 2013, ***135*** (19), 7214-7222.
5. Jensen, G. V.; Lund, R.; Gummel, J.; Narayanan, T.; Pedersen, J. S., *Angew. Chem.* 2014, ***126*** (43), 11708-11712.
6. Jusufi, A.; LeBard, D. N.; Levine, B. G.; Klein, M. L., *J. Phys. Chem. B* 2012, ***116*** (3), 987-991.
7. Kumar, V. V., *Proc. Natl. Acad. Sci. U.S.A.* 1991, ***88*** (2), 444-448.
8. Zana, R.; Talmon, Y., *Nature* 1993, ***362***, 228.
9. Larpent, C.; Laplace, A.; Zemb, T., *Angew. Chem. Int. Ed.* 2004, ***43*** (24), 3163-3167.
10. Yan, Y.; Xiong, W.; Li, X.; Lu, T.; Huang, J.; Li, Z.; Fu, H., *J. Phys. Chem. B* 2007, ***111*** (9), 2225-2230.
11. Thota, B. N. S.; Urner, L. H.; Haag, R., *Chem. Rev.* 2016, ***116*** (4), 2079-2102.
12. Ma, S.; Hu, Y.; Wang, R., *Macromolecules* 2015, ***48*** (9), 3112-3120.
13. Nishimura, T.; Sanada, Y.; Matsuo, T.; Okobira, T.; Mylonas, E.; Yagi, N.; Sakurai, K., *Chem. Commun.* 2013, *49* (29), 3052-3054.
14. Trappmann, B.; Ludwig, K.; Radowski, M. R.; Shukla, A.; Mohr, A.; Rehage, H.; Böttcher, C.; Haag, R., *J. Am. Chem. Soc.* 2010, ***132*** (32), 11119-11124.
15. Kellermann, M.; Bauer, W.; Hirsch, A.; Schade, B.; Ludwig, K.; Böttcher, C., *Angew. Chem. Int. Ed.* 2004, ***43*** (22), 2959-2962.
16. Becherer, M. S.; Schade, B.; Böttcher, C.; Hirsch, A., *Chemistry – A European Journal* 2009, *15* (7), 1637-1648.
17. Burghardt, S.; Hirsch, A.; Schade, B.; Ludwig, K.; Böttcher, C., *Angew. Chem. Int. Ed.* 2005, ***44*** (19), 2976-2979.
18. Fujii, S.; Sanada, Y.; Nishimura, T.; Akiba, I.; Sakurai, K.; Yagi, N.; Mylonas, E., *Langmuir* 2012, ***28*** (6), 3092-3101.
19. Takahashi, R.; Matsumoto, S.; Fujii, S.; Narayanan, T.; Sakurai, K., *Angew. Chem.* 2017, ***129*** (24), 6838-6842.

20. Fujii, S.; Lee, J. H.; Takahashi, R.; Sakurai, K., *Langmuir* 2018, ***34*** (17), 5072-5078.
21. Fujii, S.; Takahashi, R.; Ha, L. J.; Sakurai, K., *Soft Matter* 2018, ***14*** (6), 875-878.
22. Miyake, R.; Fujii, S.; Lee, J. H.; Takahashi, R.; Sakurai, K., *J. Colloid Interf. Sci.* 2019, ***535***, 8-15.
23. Tarnai, T.; Gaspar, Z., *Acta Crystallogr. A* 1987, ***43*** (5), 612-616.
24. Saff, E. B.; Kuijlaars, A. B. J., *Math. Intell.* 1997, ***19*** (1), 5-11.
25. Fujii, S.; Yamada, S.; Matsumoto, S.; Kubo, G.; Yoshida, K.; Tabata, E.; Miyake, R.; Sanada, Y.; Akiba, I.; Okobira, T.; Yagi, N.; Mylonas, E.; Ohta, N.; Sekiguchi, H.; Sakurai, K., *Sci. Rep.* 2017, ***7***, 44494.
26. Glatter, O. Kratky, O., Small Angle X-ray Scattering. In Small Angle X-ray Scattering; Academic Press: London. 1982.
27. Feigin, L. A. Svergun, D. I., Structure Analysis by Small-Angle XRay and Neutron Scattering; Plenum Press: New York. 1987.
28. Borysik, A. J.; Robinson, C. V., *Langmuir* 2012, ***28*** (18), 7160-7167.
29. Wennerström, H.; Lindman, B., *Phys. Rep.* 1979, ***52*** (1), 1-86.

Table of contents

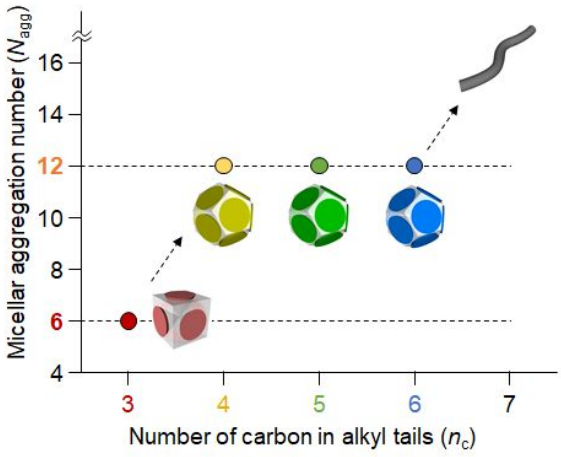

The monodisperse micellar aggregation number remains constant at 12 when increasing the alkyl chain length from C4 to C6, which is unique behaviour of Platonic micelles.